Iranian Journal of Astronomy and Astrophysics
Vol. 2, No. 1, 2015


**Iranian Journal of Astronomy and Astrophysics**

# Callibration of a homemade 4-fold Water Cherenkov Detector array, by detection of EAS events

Mehdi Khakian Ghomi[1] · Mahmood Bahmanabadi[2] · Hadi Hedayati Kh.[3]

[1] Energy engineering and physics department, Amirkabir univ. of tech., 15875-4413, Tehran, Iran. Email: khakian@aut.ac.ir
[2] Department of Physics, Sharif Univ. of Tech., 11555-9161, Tehran, Iran
[3] Department of Physics, K.N. Toosi Univ. of Tech., 15875-4416, Tehran, Iran

**Abstract**. We monitored several multi TeV EAS events by a 4-fold small array of water cherenkov detectors. The square configuration of the detectors is used for detection of secondary particles of EAS events. We logged 476,675 true EAS events by the array in a period of 9 months. With the calculation of the local coordinates $(\theta, \phi)$ of the logged events, we extracted a very good distribution of $dN/d\theta = \sin\theta(P_0 A_0 \cos\theta + p_{90} A_{90} \sin\theta)\cos^n\theta$ for the detected events with $n$=6.71±0.7. The parantese in the distribution is extracted from the water cherenkov detector geometry. By investigation of HWHM of the detector signals, we obtained a 7.2° accuracy in the direction of the EAS events. Also, we showed that the logged events are quite independent and random which is a good signature from EAS nature. Finally, we obtained 50 TeV for the threshold energy of the array with the first estimation and we obtained 95 TeV for the detection of the EAS events with a more accurate way.

*Keywords*: Extensive Air Shower, Water Cherenkov detector, Callibration of array

# 1 Introduction

In the detection of Extensive Air Shower (EAS) events, an array of scinillator detectors is usually used [1, 2, 3, 4, 5, 6]. In our previous works, we used a 4-fold scintillator detector array as a prototype for a larger one [4]. To obtain enhanced results, it is needed to have a more extended array. In our studies, we found that our optimum array should contain at least 20 detectors. Therefore, we tried to design and apply water tanks as the detectors. By passing energetic charged particles of the EAS events from the water tanks, we are able to detect cherenkov radiation inside water. Detection principle of Water Cherenkov Detectors (WCDs) is quite different from Scintillator Detectors (SDs). But both of them are sensitive to energetic charged particles. Therefore, we tried to design a complete experiment to analyse and investigate the WCDs and to compare the obtained results with SDs.
After a few tests on the WCDs itself and comparison of their results with SDs, we found that it is needed to arrange an array of the WCDs similar to the previous array for SDs [4]. In this work, we present some results from the 4-fold WCD array and show that the results are in a good agreement with an equivalent 4-fold SD array.
In the following we discuss the benefits and failure points of SDs and WCDs. Benefits of SDs are: 1- SDs are solid, so it can be used on the sloped grounds, 2- they accept less effects from environmental parameters, like air polution, air temperature and so on, 3- they have no phase transitions like freezing, evaporation or etc. 4- and they have higher densities which increase the detection probability of charged particles.
But their failure points are: 1- usually their designs are restricted by their shapes, 2- the

restriction makes some problems as like as light coverage. 3- one of the most important problems is the price of the SDs itself, which is quite expensive. 4- the last problem is specially for us; it is the import of scientific matterials for the physics laboratories, which is very hard with the sanction restrictions.
In WCDs, we have benefits of: 1- It has a good shape-forming because they contain liquid. 2- The most important material in WCDs is water; so it is very accessible and cheep. 3- Also to improve the detection efficiency, we are able to solute liquid wavelength shifter inside the water.
Failure points of WCDs are: 1- Their density is lower than the SDs. So, we need to use higher thicknesses of water as compared to SDs. 2- more impurities in water makes more conductivity and less cherenkov light, so it decreases the efficiency of particle detection in a long time. So it should be needed to conserve it from every impurities like airpolution to make its lifetime longer. 3- To improve the efficiency, it is better to change the water every 2 or 3 years once. 4- Also it needs to be used in moderate climates with no freezing or evaporation of water.
with all of the aspects for WCDs, there is a good desire to use them in EAS arrays like AUGER project.
In this work for investigation of the WCDs, we logged 476,675 true EAS events in 9 months and fitted the function $dN/d\theta = A\sin\theta(P_0A_0\cos\theta + P_{90}A_{90}\sin\theta)\cos^n\theta$ over the zenith distribution of the data, where $A_0$ and $A_{90}$ are effective surfaces for 0 and 90° zenith angle events. $P_0$ and $P_{90}$ are the detection probability of particles when they pass through these surfaces with zenith angle of 0 and 90°. These probabilities are obtained by a simulation of the WCDs geometry and cherenkov light detection inside them [7].
In previous results with flat SDs, the function $A\sin\theta\cos^n\theta$ was using over zenith angle distribution of EAS events due to their 2D geometry [4, 8, 9, 10]. From the study of different observatory results, we find that for higher sites from sea level have smaller power $n$ becomes smaller [10, 11]; which is due to the thickness of the atmosphere and specially due to the atmospheric absorbtion effects [12, 13, 14].
In what follows, we tried to do our analysis step by step.
In the second section, we explain our experimental setup and recording procedure of the EAS events. In section 3, we briefly present the callibration of our experiment. In section 4, we explain our calculations of local coordinates and analysis of their distributions. In 5th section, we calculate angular resolution of the experiment and in the next section it is calculated the energy threshold of our experiment. And finally in the last section, we have a disscusion over the comparison of WCDs and SDs.

## 2 Experimental setup

The array is constructed of 4 WCDs located at the roof of the physics department, Sharif University of Technology, 51° 20′ E and 35° 43′ N, elevation 1200 m a.s.l. (890 g cm$^{-2}$) in Tehran (Fig. 1(a)) which is the prototype of ALBORZ observatory at the elevation of 2650 m a.s.l. (http://observatory.sharif.ir). Our detectors are on a flat horizontal surface. Each detector is a cylindrical metalic reservoir with 64 cm diameter and 1.2 m height. Configuration of the array is 6.08×6.08 m$^2$ centre by centre. The interior surface of each detector is coated with white paint because of the best reflectivity and efficiency [3], a 52 mm EMI 9813B PMT is used with its face inside the water. If at least one particle passes through the detector, the PMT creates a signal with a pulse height related to direction, kind of the passed particle, and length of the particle track, inside water [7]. Wavelength of the Cherenkov Radiation in stealed water is about 470 nm [15], and amplification coefficient of

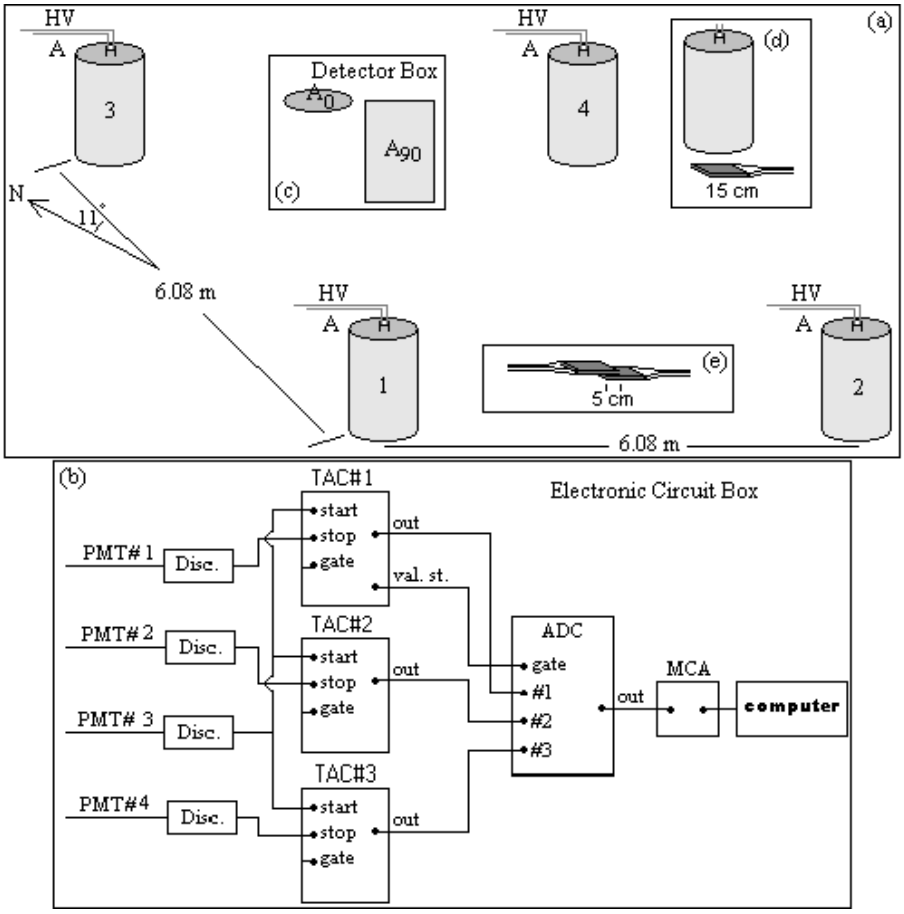


Figure 1: Different parts of the figure respectively show (a): schematic configuration of our detector array, (b): data acquisition system and used electronic circuits, (c), (inside a): vertical ($A_0$) and horizontal ($A_{90}$) sections of our detectors (d), (inside a): Experimental arrangement for study of zenith events in WCDs (e), (inside a): Experimental arrangement for calibration of the reference SD

the PMT in this wavelength is about $10^8$ (www.electronictubes.com). For the detection of the EAS events, it was used an electronic circuit with NIM modules (Fig. 1(b)). It was used 4 fast discriminators (CAEN N413A) which is operated at fixed levels of 35 mV to 200 mV. The threshold of each discriminator is set in order to separate signal and background noise levels. The discriminator outputs are connected to three Time to Amplitude Converters (TACs)(EG&G ORTEC 566) which are set to a full scale of 200ns (maximum acceptable time difference between each two WCDs). $\Delta t_{31}$, $\Delta t_{32}$ and $\Delta t_{34}$ (are fed into TACs 1 to 3 respectively) and $T_{GMT}$ the three time differences between the four WCDs and true time (GMT) of each EAS event. Then, the three TAC outputs are fed into a multi-parameter Multi Channel Analyzer (MCA)(KIAN AFROUZ Inc.) via an Analogue to Digital Converter (ADC)(KIAN AFROUZ Inc.) unit as parameters 1 to 3. The trigger condition is only on parameter 1. It means that if parameter 1 turns on, it will be recorded the event. Since the array is a 4-fold simple array, it is put the selection of the data to the offline part.

Usually in the large arrays, there is some problems with the very large amount of recorded data not only on the recorded memory, but also on the process of the offline selection of the real data. Since we didn't have the problems because of the smallness of the array, we applied a soft trigger condition and recorded more events. Because sometimes hard trigger condition eliminates few percent of the true real data too. Also the soft trigger condition is due to the simplicity of the logic and using less electronic modules. In this case, we get rid of some hardware problems of the logic unit modules. Therefore, we have to eliminate a part of the recorded data which are useless because of the soft trigger condition. For example, a uselesss event is when one, two or three of the 4 WCDs has no signals. After this refinement, we eliminate most of the useless recorded data. In 30 runs, we obtained 1,768,195 recorded events in 12,258,670.0 seconds and after two steps of refinement, we obtained the fine number of events 476,675 with the obtained rate equal to 0.0389 Hz.
Since the WCDs have cylindrical shapes, the effective surface of the detectors depends on zenith angle of EAS events. The effective surface is $A_{eff} = P_0 A_0 \cos\theta + P_{90} A_{90} \sin\theta$ (Fig. 1(c)(inside 1(a))). Therefore, we should apply $dN/d\theta = A \sin\theta (P_0 A_0 \cos\theta + P_{90} A_{90} \sin\theta) \cos^n \theta$ for zenith angle distribution of the events. The $\sin\theta$ is due to solid angle and $(P_0 A_0 \cos\theta + P_{90} A_{90} \sin\theta)$ due to the effective cross sectionof WCDs for particles in passing through them. The $\cos^n \theta$ is due to the absorbtion effect of the the atmosphere on the EAS events.

# 3 Data Callibrations

## 3.1 EAS arrival GMT and time syncronization

It is synchronized (http://www.timeanddate.com) our computer and electronic systems to GMT with recording capability of 20 $Hz$. If an EAS event occurs, its three time lags will be recorded and if it does not occur, 'zero' will be recorded. Therefore, the starting time of each run and the count of records gives us the GMT of each EAS event. Since the time differences of signals from two detectors must not be larger than $d/c$, so we selected two elliptical islands of data between $\Delta t_{31}\&\Delta t_{32}$ and, between $\Delta t_{32}\&\Delta t_{34}$ and one circular island between $\Delta t_{31}\&\Delta t_{34}$. For a complementary explanation about the islands, it should be suggested that the time between the two WCDs must not be larger than the distace between the two WCDs divided by the speed of light. Therefore, for the $\Delta t_{31}\&\Delta t_{34}$ which both of them is on the sides of the square (Fig. 1(a)) with equal maximum time intervals; therefore the island will be a circle. In other cases ($\Delta t_{31}\&\Delta t_{32}$ and $\Delta t_{32}\&\Delta t_{34}$) which one of them are on the diameter, the islands have eliptical shapes. After the discrimination a new smaller data set has been selected (476,675 EAS events from 496,015 logged events fall in the islands), the new date set is used to reconstruct the arrival direction of the EAS events.

## 3.2 Timing calibration correction

Electronical recorded time delays of the logged events consist of 2 independent parts. The first one is the geometry of each WCD itself; and the second one is the electronic support of each WCD. In this investigation, we applied a unique support electronic for all of the WCDs to avoid any difference between the WCDs. We found the delay time for each WCD itself by comparing it with a reference SD. For timing-calibration of the detectors, it is measured systematical time-offset among different detectors. These systematical time offsets are due to difference in cable lengths, electronic modules, geometry of each WCD and so on. For the calibration of the detectors in our array, we proceeded as follows :

We used a reference detector (A plastic scintillator 15×15 cm$^2$). We put the reference SD ($SD_R$) close to each $WCD_i$ ($i$ = 1..4) and measured the mean time difference $T_{Ri}$. We obtained the mean time differences $a_1$, $a_2$, $a_3$ and $a_4$ in nanoseconds for $WCD_1$ to $WCD_4$ and the $SD_R$. For the $SD_R$ and all WCDs, it is used the same cable and electronic supports.
The corrections $T_{R1}$, $T_{R2}$, $T_{R3}$ and $T_{R4}$ for WCDs 1 to 4 are 0.77, -0.14, 0.00 and 0.10 nanoseconds, respectively. We put $T_{R3}$ = 0.00 manually, since we used the WCD3 as reference for the WCDs.
Then we applied the callibration of the detectors on each WCD time callibrated as follows: $T_{i3}^{mesrd} = T_i^{mesrd} - T_3^{mesrd} = (T_i^{exact} + T_{Ri}) - (T_3^{exact} + T_{R3}) = \Delta T_{i3}^{exact} + T_{Ri}$

# 4 Calculation of Local coordinates ($\theta$,$\phi$) and direction cosines ($l$,$m$) by least square method

The local coordinates zenith ($\theta$) and azimuth ($\varphi$) in our detection procedure are calculated based on the time differences between WCDs [16] and least square method [17]. It is assumed that the shower front could be approximated by a plane. So we obtain,

$$\tan\theta = \sqrt{\frac{X^2+Y^2}{1-X^2-Y^2}} \quad , \quad \tan\varphi = Y/X \tag{1}$$

where,

$$X = c \begin{vmatrix} \sum x_{3j}t_{3j} & \sum x_{3j}y_{3j} \\ \sum y_{3j}t_{3j} & \sum y_{3j}^2 \end{vmatrix} \Big/ \begin{vmatrix} \sum x_{3j}^2 & \sum x_{3j}y_{3j} \\ \sum x_{3j}y_{3j} & \sum y_{3j}^2 \end{vmatrix} , \tag{2}$$

$$Y = c \begin{vmatrix} \sum y_{3j}t_{3j} & \sum x_{3j}y_{3j} \\ \sum x_{3j}t_{3j} & \sum x_{3j}^2 \end{vmatrix} \Big/ \begin{vmatrix} \sum x_{3j}^2 & \sum x_{3j}y_{3j} \\ \sum x_{3j}y_{3j} & \sum y_{3j}^2 \end{vmatrix} . \tag{3}$$

$j = 1, 2, 4$, $\mathbf{D_{3j}} = \mathbf{D_j} - \mathbf{D_3} = x_{3j}\hat{\mathbf{i}} + y_{3j}\hat{\mathbf{j}}$ and $t_{3j} = t_j - t_3 + T_{j3}^{exact}$ are respectively the coordinate vector and the time lag of $j_{th}$ detector with respect to the reference one (detector #3) and $c$ is the speed of light.
A zenith angle cut off of 60° is implemented to enhance more reliable results. In Fig. 2(a), it is shown that the zenith distribution of the experiment has a coincidence with the $dN/d\theta$ with $n = 6.80 \pm 0.7$.

Since we need to compare our results with the results of other experiments or cosmic ray simulation codes, we divided each 5 degree intervals (i to f) to $\int_i^f \sin\theta(P_0 A_0 \cos\theta + P_{90} A_{90} \sin\theta) d\theta$ to eliminate the geometrical effects. The function $dN/d\theta = A_1 \cos^n\theta$ has been fitted on the resulting distribution with $n = 6.71 \pm 0.7$ (Fig 2(b)); which only consists of the absorbtion effect.
Fig. 2(c) shows the azimuthal distribution of the EAS events which is in agreement with the following anisotropy function $D(\phi)$ :

$$D(\phi) = \alpha_0 + \alpha_1 \cos(\phi - \alpha_2) + \alpha_3 \cos(2\phi - \alpha_4) \tag{4}$$

where $\alpha_0$ to $\alpha_4$ are respectively 45161, 3292, 180, 1259, 39.
Also we calculated the direction cosines $l = \sin\theta\cos\phi$ and $m = \sin\theta\sin\phi$ for each EAS event and obtained the distributions for the $l$ and $m$. With fitting the gaussian function on these two distributions, we obtained the mean $\bar{l} \pm \sigma_l$ and $\bar{m} \pm \sigma_m$ equal to -0.0093±0.3937 and -0.0107±0.3855 for $l$ and $m$ respectively which are very near to zero. It shows that there is no prefered direction in our detected events.

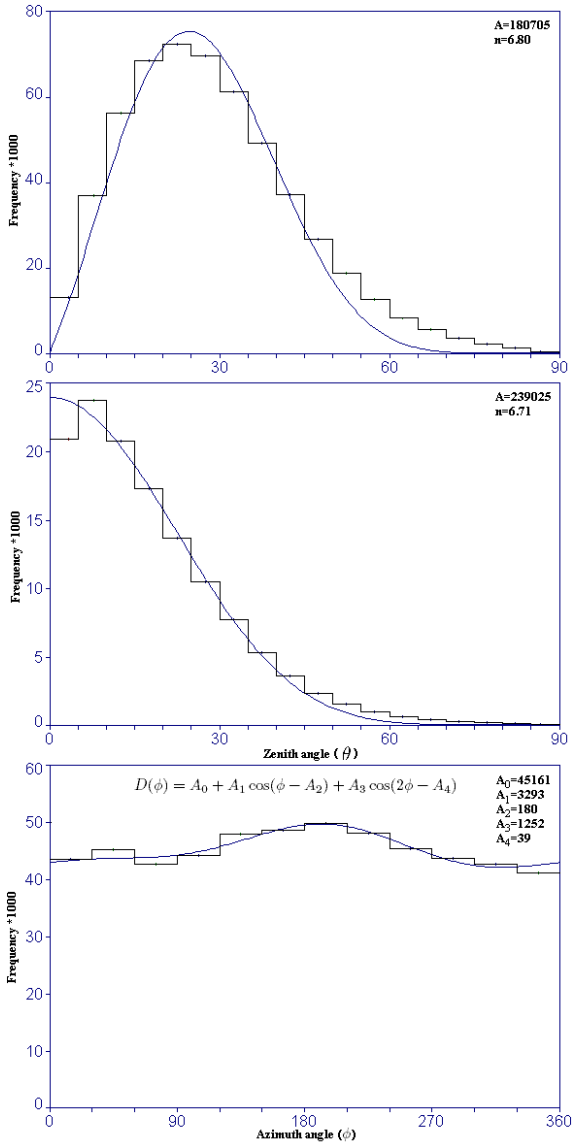


Figure 2: The curves show respectively (a): the zenith distribution of 476,675 logged EAS events which is fitted with the function $dN/d\theta$ with $n = 6.80$ and (b): the upper distribution divided by $2\pi \int_i^f \sin\theta(P_0 A_0 \cos\theta + p_{90} A_{90} \sin\theta)d\theta$ for comparison with the simulated results and $n = 6.71$. (c): Distribution of azimuth angles of the logged EAS events.

# 5 Calculation of angular resolution of the experiment

Angular resolution is one of the most important identifications of each experiment, which it should be estimated.
The time difference between each two WCDs idealy is due to the distance between the two detectors and also the direction of the event. So at first it should be restricted the logged events in a very short range of angles. Therefore, we put a small SD (reference 15×15 $cm^2$) exactly under each WCD (Fig. 1(d)). Therefore, most of the detected events by the setup are zenith events. The time difference, between the WCD and the SD ideally should be due to the distance between them. But not only the WCD, but also the SD have uncertainties in their detection times. When we obtained the distribution of the time differences it should be a gaussian distribution with the centre of the ideal time difference and a Half Width Half Maximum ($\sigma$). The $\sigma$ consists of two uncertainties from the WCD and the SD ($\sigma^2 = \sigma^2_{WCD} + \sigma^2_{SD}$).
We obtained the $HWHMs$ of the time differences $HWHM_1$ to $HWHM_4$ for WCD1 to WCD4 with the reference detector respectively. It was said before that, in all of the callibration procedures it was said before that in all of the callibration processes a unique cable and electronic support were used for the reference detector; and also a unique electronic support for each of the 4 WCDs. To determine the contribution of the reference detector in the *HWHMs* of the time differences, we used a similar scintillator over the reference one with only 5 cm superposition of the end of each scintillator for limiting the effective scintillation zone (Fig. 1(e)). It means that the logged events pass through the 5 cm of the end of each scintillators width. In this setup the $\sigma^2 = \sigma^2_{SD} + \sigma^2_{SD} = 2\sigma^2_{SD}$; therefore, HWHM of each reference detector is $HWHM_{mesrd}/\sqrt{2}$. Then, we obtained $HWHM$ of the time difference $T_{RR'}$=6.18 nanoseconds.
In this step by the separation of the error contribution of all WCDs , we found mean amount of 6.56±0.20 nanoseconds for $\bar{H}WHM$ of the $WCD_i$. Therefore with the eqs. 1, 2 and 3 for $\theta$ and $\phi$ and error propagation procedure we found the angular error of $7.2^{\pm}1.0^{\circ}$ for the configuration.

# 6 Calculation of energy Threshold of the experiment

Since we are not able to measure the energy of air showers on event by event basis, so it has to be obtained the energy threshold of the experiment by comparing of the experimental results with the simulated results and also by the analysis of recording rate.
To obtain the Threshold Energy of the experiment ($E_{th}$), it is needed to calculate the effective solid angle $\Omega = \int_0^{2\pi}\int_0^{\pi/3} \sin\theta d\theta d\phi = \pi$ sr, event rate and effective surface of the experiment ($S_{eff}$).

## 6.1 Calculation of the event rate

For the event rate of the experiment in 30 runs, equivalent to a total of 12,258,670.0 seconds, the number of 476,675 true EAS events were recorded, and thus the rough rate obtained 0.0389 Hz. To obtain the event rate more accurately we extracted the time differences ($\Delta t_1$) between each two consecutive events, since these time differences are quite random, the distribution of the time differences has had a very good agreement with an exponential distribution $F(\lambda_1) = Ae^{(-\lambda_1 \Delta t_1)}$ with the rate coefficient $\lambda_1 = 0.0391$ Hz (Fig. 3(a)).

Also the time differences ($\Delta t_m = t_i - t_{i-m}$) between each ($m =$) 3, 4, 5 and 6 sequential events were extracted (Fig. 3(b)). Since these events are quite random, these distributions

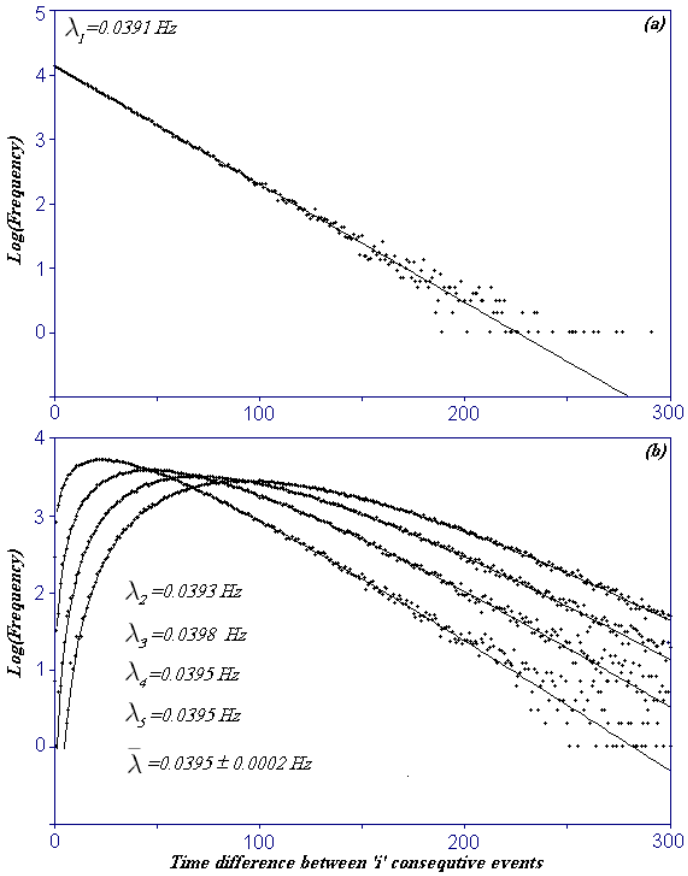


Figure 3: a) The fitted exponential function on the true time(GMT) differences of each two following events, the obtained rate is 0.0391 Hz, b) the time differences between 3, 4, 5 and 6 sequential events.

have very good agreement with gamma function :

$$G(\Delta t_m, \lambda_m, m) = \frac{\Delta t_m^{m-1}}{(m-1)!} N \lambda_m^m \exp(-\lambda_m \Delta t_m) \tag{5}$$

which $\lambda_m$ is the rate with $m$ from 3 to 6. The different values of $\lambda_m$ are compatible with each other and the mean value is $\bar{\lambda} = 0.0395 \pm 0.0002$ Hz.

### 6.2 Calculation of effective surface of the array

For a rough estimation of the smallest energy of each EAS event, it is assumed that the front of the EAS event is the smallest circle which cover the 4 WCDs. So we have a circle at least with the diamiter equal to the diameter of the square, with $S_{eff} \approx$50 m$^2$.
To have a better estimation, we simulated 114,341 EAS events with CORSIKA code [18]. Since the trigger condition of the logged events is passig at least one charged particle from each detector, so it should be applied the condition as follows:
At first, we should find the effective surface of each detector.

$$\bar{A}_{eff} = \frac{\int_0^{\pi/3} (P_0 A_0 \cos\theta + P_{90} A_{90} \sin\theta) \sin\theta d\theta}{\int_0^{\pi/3} \sin\theta d\theta} = 0.71 \text{ m}^2. \tag{6}$$

Since for the particle detection at least one particle is sufficient for the motivation of the WCD, so it can be detected at least $\rho_r$=1 particle/$\bar{A}_{eff}$. Then, we distributed the secondary particles of the EAS events on 100 concentric circles with the radial difference of 0.2 m. Also we divided the number of the secondary particles of each ring zone to its surface. Finally, it was obtained a distribution of radial density of secondary particles vs. $r$ ($\rho(r)$). From the $\rho(r)$, it was found that at $r = 6.6\,m$ the $\rho(r) = 1\,particle/\bar{A}_{eff}$, and we found $S_{eff} = 137\,m^2$.

### 6.3 Energy threshold calculation

By two different $S_{eff}^{Rough}$ and $S_{eff}^{Simulated}$ it is obtained $E_{th}^{Rough} = 58$ TeV and $E_{th}^{Simulated} = 106$ TeV by Hillas formula [19] respectively.

$$F(>E) \sim 2 \times 10^{-10} \frac{\text{particle}}{\text{cm}^2 \text{ s sr}} \times (\frac{E}{1000 \text{ TeV}})^{-\gamma} \tag{7}$$

By using Borione flux [20], $\bar{\lambda}$, $\Omega$ and $S_{eff}^{Rough}$ and $S_{eff}^{Simulated}$ :

$$J(E) = 2.78 \times 10^{-5} E^{-2.22} + 9.66 \times 10^{-6} E^{-1.62} - 1.94 \times 10^{-12} \quad 40 \leq E \leq 5000 \text{ TeV} \tag{8}$$

it is obtained $E_{th}^{Rough} = 46$ TeV and $E_{th}^{Simulated} = 83$ TeV which is not so far from the result obtained from Hillas formula.

## 7 Conclusion

In this work, it was tried to develop WCDs to apply them instead of SDs. Fortunately, the results in the logged and analized data sets, shows a good agreement between the WCDs and SDs.

At first, it was syncronized the computer and electronic system with GMT, then callibrated the systematic time errors between the WCDs by a reference detector. In the following, the randomness and truth of the data set was chacked, and also obtained the local coordinates ($\theta$ and $\phi$) distributions which are in a good agreement with SDs.
Of course in the $\theta$ distribution, there is a meaningful difference between WCDs and SDs. In SDs $n = 5.58$ but in WCDs $n = 6.71 \pm 0.7$; which shows that WCDs are less sensitive to more zenith events. This subject is quite logical due to the geometry of the WCDs with respect to SDs. Zenith events with small $\theta$ traverse vertical length of the WCD, but inclined events pass through the diameter of the WCD. So path length of the particles are smaller for inclined events. Therefore, the detection probability is less sensitive in higher zenith angles.
Finally, it was obtained a rough estimation for threshold energy of the WCD array which is about 50 TeV, and then obtained a simulated threshold energy about 95 TeV. In the reference [4] with SD array, it was estimated their threshold energy as like as our rough estimation and they obtained about 50 TeV for thir 4-fold arry of SDs.
At the end, it should be suggested that, the WCD array has a failure point respect to the similar SD array. The SD array had an angular resolution of about $4.35 \pm 0.85^\circ$ [4] and the WCD array had the resolution $7.2 \pm 1.0^\circ$. It is because of the long path of the passed particle through the WCDs in case that the particle path through SDs is very small. Of course, it should be mentioned that, the array should be able to improve the angular resolution by using more WCDs and the result is obtaind from only a 4-fold one.
With all of the considerations and these results, it is shown that the WCDs are good candidates to use in place of the SDs for detection of EAS events.

## Acknowledgment

This research was supported by a grant from the national research console of Iran for basic sciences.
M. Khakian acknowledges University of Lecce, ARGO-YBJ group and INFN for a three month grant to a fruitful visit there. I learned some of the applied thechniques in this work in the collaboration with the university

## References

[1] S. Abdollahi, M. Bahmanabadi, et.al. (2015), arXiv, 150100110A

[2] M. Bahmanabadi, F. Sheidaei, M. Khakian Ghomi and J. Samimi, Phys. Rev. D 74 (2006), 08

[3] M. Bahmanabadi, A. Anvari, G. Rastegarzadeh, J. Samimi, and M. Lamehi Rachti, Experimental Astronomy 8/3 (1998), 211

[4] M. Khakian Ghomi, M. Bahmanabadi and J. Samimi, A&A 434 (2005), 459

[5] A.V. Glushkov, M.I. Pravdin, A. Sabourov, Phys. Rev. D, (2014), Vol. 90, id012005

[6] S.K. Gupta, et.al., Experimental Astronomy, 35 (2013), 507-526

[7] F. Sheidaei, M. Bahmanabadi, A. Keivani, M. Khakian Ghomi, A. Shadkam and J. Samimi, Physical Rev. D, (2007), Vol 76, 082002

[8] M. Bahmanabadi, M. Khakian Ghomi, J. Samimi and D. Pourmohamma, Experimental Astronomy 15/1 (2003), 13

[9] M. Bahmanabadi, A. Anvari, M. Khakian Ghomi, J. Samimi and M. Lamehi Rachti, Experimental Astronomy 13/1 (2004), 39

[10] S. Luori and M.M. Winn, NIM A223 (1984), 173

[11] S.M.H. Halataei, M. Bahmanabadi, M. Khakian Ghomi, J. Samimi, *Physical Rev. D*, 77, 8, 083001 (2008)

[12] P. Bernardini, I. De Mitri and G. Marcella et al. 29th ICRC 6 (2005), 153

[13] A. De. Angelis and O. Mansutti, *Energy Gamma Ray Experiments* (Proceeding of the 3rd workshop on:, 2005)

[14] L.I. Dorman, *Cosmic rays in the earth's atmosphere and underground* (Cluwer Academic Publisher, 2004)

[15] C. Grupen, *Astroparticle Physics* (Springer, 2005)

[16] P. Sokolsky, *Introduction to Ultra High Energy Cosmic Ray Physics* (Adison-Wesley publishing company Inc, 1989)

[17] K. Mitsui *et al.*, NIM A290 (1990), 565

[18] Hech, D., et al., report **FZKA6019**(1998), Forschungszentrum Karlsruhe; http : //www − ik.fzk.de/corsika/physics$_{d}$escription/corsika$_{p}$hys.html.

[19] K. Greisen Ann. Rev. Nuc. 10 (2005), 63

[20] A. Borione, M.L. Catanese, M.C. Chantel *et al.* ApJ 481 (1997), 313